

The test and calibration system for the Elementary Cells of the Cherenkov Camera in the PBR Mission

Rossella Caruso^a on behalf of the JEM-EUSO Collaboration

(a complete list of authors can be found at the end of the proceedings)

^a*Department of Physics and Astronomy “E.Majorana”, University of Catania and INFN-Catania,
Via Santa Sofia 64, 95123 Catania, Italy*

E-mail: rossella.caruso@dfa.unict.it, rossella.caruso@ct.infn.it

The development of detectors using Silicon Photo-Multipliers for acquisition of fast light signals coming from Cherenkov and fluorescence emissions started by particle showers in the terrestrial atmosphere is the main goal of the Italian ASI/INFN Agreement n.2021-8-HH.2-2022, named “ASI/INFN_EUSO-SPB2”, in view of the next generation of telescopes in balloon-borne and space-based experiments. A survey of performances of different Silicon Photo-Multipliers available on the market has been performed to identify the best sensors for space applications, where high thermal excursions and environmental radiation must be mainly taken into account in contrast to ground-based experiments. In particular, a characterization protocol for Silicon Photo-Multiplier qualification has been specified to Hamamatsu S13161-3050AE-08 sensor (8×8) array in the 30 C° down to -40 C° temperature range. The protocol specifies measurements of breakdown voltage, quenching resistance, gain, dark count rate and the probability of cross-talk. These parameters have been measured as a function of temperature at fixed over-voltage. Based on these previous measurements, a dedicated set-up is under completion for performing massive tests to validate and calibrate 32 Silicon Photo-Multipliers (Hamamatsu S13361-3050 series, 64 channels each), composing the (2048 pixels, $12^\circ \times 6^\circ$ field of view) Focal Surface of the Cherenkov Camera that will fly on the POEMMA-Balloon with Radio mission. The technical details and description of this system and the procedural steps implemented are reported, preliminary measurements on the first Elementary Cell are also shown.

1. Preface

In the last years, novel semiconductor photo-detectors, such as Silicon Photo-Multipliers (SiPMs) (see Sec.2), have been developed for fundamental science experiments, constituting the enabling technology for a diverse and rapidly growing range of applications: experimental physics, medical imaging and commercial applications are only a few examples. In the recent period, especially, in the framework of the astroparticle physics, an intense investigation of using SiPMs in space applications is ongoing for the next generation of telescopes in balloon-borne and space-based experiments. In the present contribution, a preparatory phase (see Sec.3), devoted to the development of detectors based on Silicon photo-sensors for acquisition of fast light signals coming from Cherenkov and fluorescence emissions started by charged particles during the development of the Extensive Air Showers (EAS) in the Earth's atmosphere, is introduced. It represents the base for an implementation in Cherenkov and Fluorescence telescopes of the JEM-EUSO Program and, specifically, for the next intermediate sub-orbital mission, named POEMMA Balloon with Radio (PBR) (see Sec.4).

2. Pearls and pitfalls of using SiPMs as photo-detectors in space-based experiments

A SiPM is composed of a matrix of identical micro-cells, each one consisting of a so-called Geiger-mode Avalanche Photo-diode (G-APD) or Single-Photon Avalanche Diodes (SPAD) and a quenching resistor (R_q) connected in series. The micro-cells are connected in parallel to a bias voltage (V_{bias}). SiPMs are also known as Multi-Pixel Photon Counters (MPPCs), naming a micro-cell as pixel. Every pixel produces the same signal when it is hit by a photon and the sum of the pixel responses gives the channel output. The typical dimension of a SiPM sensor is between $(1 \times 1) \text{ mm}^2 \div (6 \times 6) \text{ mm}^2$ and the number of micro-cells per device ranges from several hundreds to several tens of thousands. Micro-cells vary between $(10 \times 10) \mu\text{m}^2 \div (100 \times 100) \mu\text{m}^2$ in size, as an example: Hamamatsu S13161-3050AE-08 with channel of $(6 \times 6) \text{ mm}^2$ and micro-cell $(50 \times 50) \mu\text{m}^2$ [1], [2]. SiPMs offer numerous advantages over conventional vacuum tube Photo-Multiplier Tubes (PMTs), such as:

- **solid-state technology**: they are solid-state devices, meaning they are more resistant to mechanical shocks, vibrations, and extreme temperatures, which is beneficial for harshest environments;
- **compact size and low voltage operation**: they are significantly smaller and require much lower operating voltages (10 \div 100 times lower than PMTs), simplifying electronics and reducing power consumption;
- **cost-effectiveness**: the mass production of Silicon electronics makes them generally less expensive;
- **modularity**: they present an opportunity for constructing modular detectors surfaces due to their compact and lightweight design. To build large sensitive areas, SiPMs can be arranged in arrays;
- **magnetic field immunity**: they are largely unaffected by magnetic fields;
- **high Photon Detection Efficiency (PDE)**: in the red to near-infrared range, they can achieve higher quantum efficiencies than available PMT photocathode materials;
- **large Gain (G) and output signal**: they provide a high gain and a large output signal, capable of detecting single photons;

- **low excess noise factor:** they often have a more deterministic photo-electron gain, leading to a lower or negligible excess noise factor and potentially a better signal-to-noise ratio;
- **dynamic range:** by using large arrays of SiPMs, their dynamic range can be significantly expanded, allowing for faster imaging rates or higher signal-to-noise ratios without saturation issues. Nevertheless, SiPMs are usually more sensitive to the temperature and present also other disadvantages, such as:
 - **cost and area:** while generally cheaper for smaller areas, the cost per unit area of SiPMs can be comparable to or even higher than PMTs for larger detection areas;
 - **high Dark Count Rate (DCR):** they exhibit a significantly higher DCR, which can be problematic in low-light applications. DCR is also highly dependent on temperature, requiring cooling for optimal performance;
 - **radiation sensitivity:** they are susceptible to radiation damage, particularly from displacement damage caused by high-energy hadrons, leading to an increase in DCR and degradation of performance over time;
 - **probability Cross-Talk (pCT):** the phenomenon where a single photon can trigger a cascade effect that fires multiple micro-cells within the SiPM, leading to increased noise and reduced signal-to-noise ratio;
 - **limited dynamic range and band-width:** the limited dynamic range of SiPMs can cause non-linear distortions in the received signal at higher light intensities, and their limited band-width can restrict the maximum transmission rate in certain applications;
 - **sensitivity below 400 nm and higher wavelengths:** while some SiPMs have improved near-Ultra-Violet sensitivity, traditional SiPMs are not highly sensitive below 400 nm (where Cherenkov light is emitted) but are too sensitive at higher wavelengths, increasing susceptibility to night sky background noise.

The design, assembly and completion of a telescope for space applications based on a focal surface formed by arrays of SiPMs must take into account all the above-mentioned factors and achieves a proper balance among pearls and pitfalls of SiPMs.

3. The preparatory phase of the ASI/INFN_EUSO-SPB2 Project

The development of detectors based on SiPM photosensors for acquisition of fast signals coming from Cherenkov and fluorescence emission started by EASs in the atmosphere, is the main goal of the current ASI/INFN Agreement n.2021-8-HH.2-2022 and its following amendments and agreements, signed between the Italian Space Agency (ASI) and the National Institute of Nuclear Physics (INFN), named “ASI/INFN_EUSO-SPB2 (Extreme Universe Space Observatory - Super Pressure Balloon 2)”. It is devoted to the design, development, advancement, production and completion of a Cherenkov and/or Fluorescence telescope prototype for the next generation of balloon-borne and space-based experiments, with the ultimate purpose of enhancing the Technology Readiness Level (TRL) of such technique. In such framework, the study of performances of different SiPMs available on the market has been performed to identify the best sensors for space applications, where high thermal excursions and environmental radiation must be mainly taken into account with respect to ground-based experiment for indirect measurements of Ultra-High-Energy Cosmic Rays (UHECRs). A specific Working Package (WP), identified as *WP4400:Characterization, selection*

and validation of SiPMs has been based on the definition of a procedure in order to characterize and select the SiPM sensors that best fit experimental requirements for space applications. The most important outcome of a long research activity on various SiPMs was a complete study concerning an (8×8) SiPM matrix (Hamamatsu S13360-3050AE-08) [3], showing the best performances over a wide range of temperatures by evaluating the R_q , the V_{bd} break-down voltage, the G , the pCT and the DCR. Two different configurations were adopted (see fig.1): the first used a pico-ammeter to measure accurately the leakage currents in order to determine the V_{bd} and R_q by means of the I current and V voltages (I - V) curves, both in *forward* and *reverse* modes, and the second one adopted a CAEN DT5202 Front-End and Read-out System (FERS) device to evaluate G , DCR and pCT by means of the multi-peak spectrum. [4], [5].

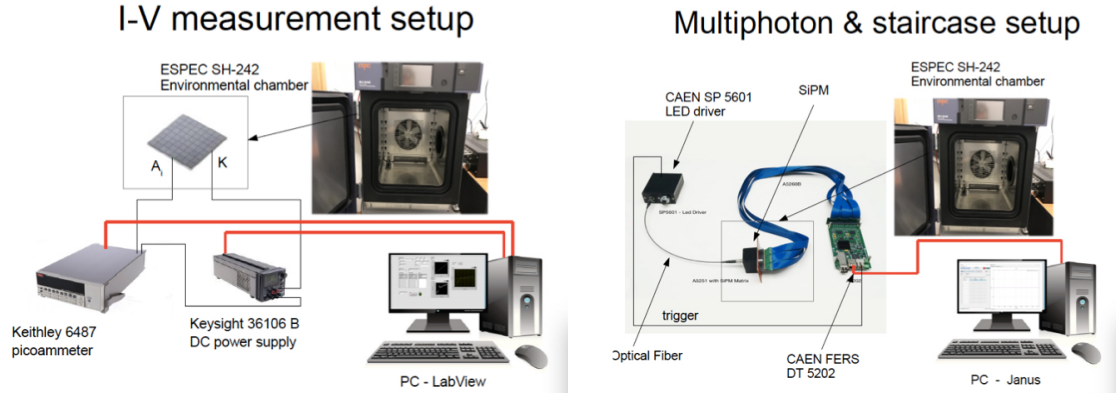


Figure 1: Left: the experimental set-up for measuring the SiPM ($I - V$) curves at different temperatures. Right: the experimental set-up for measuring the SiPM multi-peak spectrum at different temperatures.

4. The JEM-EUSO Program and the PBR mission

Since 2010, the international JEM-EUSO (Joint Exploratory Missions for Extreme Universe Space Observatory) Collaboration (URL: <https://www.jemeuso.org>), around 170 researchers, 60 institutions and 16 countries has been developing an ambitious Program ([6], [7]) with the support of major International and National Space Agencies (ASI, CNES, ESA, JAXA, NASA, ROSCOMOS) and research funding institutions, to enable UHECR ($E > 100$ PeV) and Very High-Energy (VHE) neutrino ($E > 1$ PeV) observations from space. Its main objective is to develop a large mission with dedicated instrumentation looking down on the Earth's atmosphere from space, both towards nadir and/or towards the limb direction, to detect the EAS initiated by such particles in the high atmosphere. This strategy is intended to complement the observations made with ground-based observatories by allowing a significant increase in the exposure and by achieving near-uniform full sky coverage. In the last decade, the JEM-EUSO Collaboration effectively developed five intermediate missions: one ground based (EUSO-TA [8]), three balloon-borne (EUSO-Balloon [9], EUSO-SPB1 [10], EUSO-SPB2 [11] and one space-based (Mini-EUSO [12],[13])). Recently, a new balloon-borne flight has been approved and funded by NASA for a launch planned in Spring 2027 from the Wanaka base in New Zealand. This next intermediate mission, PBR ([14]), will be the closest prototype to date for the large-size space-based POEMMA (Probe Of Extreme Multi-

Messenger Astrophysics) mission [15], a stereo double telescope to be considered for a NASA Probe Mission in the next decade. The PBR Mission is a scientific mission involving an instrument designed to be carried by a NASA suborbital Super Pressure Balloon (SPB) with a projected duration of up to 100 days, circling over the Southern Ocean. The PBR instrument consists of a 1.1 m aperture Schmidt telescope [16], similar to the POEMMA, with two photo-detectors in its hybrid Focal Surface (FS): a Fluorescence Camera (FC) [18] and a Cherenkov Camera (CC) [19], both mounted on a frame that can be tilted [17] to point from nadir up to 13 degrees above the horizon. In addition, PBR has a Radio Instrument (RI) optimized for the detection of EASs, covering the (50 \div 550) MHz range.

5. The calibration system of the Elementary Cell units and first results

The Focal Surface (see fig.2) of the PBR Camera Cherenkov (CC) contains four rows of 8 Elementary Cells (ECs). Each EC is a “sandwich” (see fig.2) composed by a SiPM (8×8 channels) matrix, a custom Printed Circuit Board (PCB), supporting two LSHM-120-02.5-L-DV-A-S-TR Samtec high-speed connectors (2 rows, 40 positions) and a 3D printed spacer, joined by means of M1 screws. Two (40 positions) HLCM-20-12.00-TD-TH1 Samtec 38 AWG micro-coax cables connect the EC to the Front-End and Read-out electronics. Each SiPMs matrix is an Hamamatsu (S13361-3050AE-08 model) photo-sensor, with specific properties reported in fig.3, consisting of 64 channels of (3×3) mm² pixels, totaling 32 SiPM matrixes and 2048 pixels for the entire camera. Each row (8 ECs, 512 pixels) constitute a CC Photo Detection Module (or CC-PDM). These CC-PDMs are mounted on a structure that shapes the photo-sensitive plane to approximate the spherical curvature required by the telescope optics. The total FoV spans ($12^\circ \times 6^\circ$), with each pixel covering 0.2° . The sensitive wavelength range is (320 \div 900) nm. The Read-Out electronics will be either based on RadioROC or MIZAR ASICs [20], which are under development by providing a sampling frequency of 200 MHz.

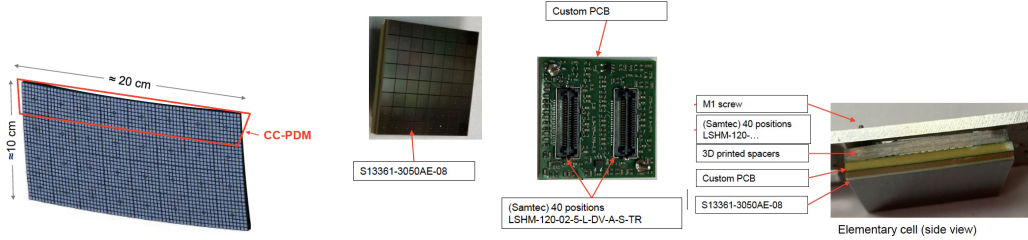


Figure 2: From left to right: an artistic view of the Focal Surface; different components of an Elementary Cell.

A characterization protocol for the EC qualification in the 30 C° down to -40 C° temperature range has been specified. The protocol specifies measurements of V_{bd} , R_q , G , DCR and the pCT. These key parameters can be measured as a function of temperature at fixed V_{ov} for each channel of each EC. A dedicated experimental system - composed by two different set-ups, one for SiPMs measurements of ($I - V$) curves and the other for SiPMs measurements of multi-peak spectra (see fig.4) - has been recently finalized for performing massive tests to test and calibrate the 32 Electronic Cells, one at a time. Both set-ups make use of an SH-242 environmental chamber produced by ESPEC hosting the EC, to perform tests at stable and different temperatures. This chamber spans ($-40 \div +150$) $\pm 0.5^\circ\text{C}$

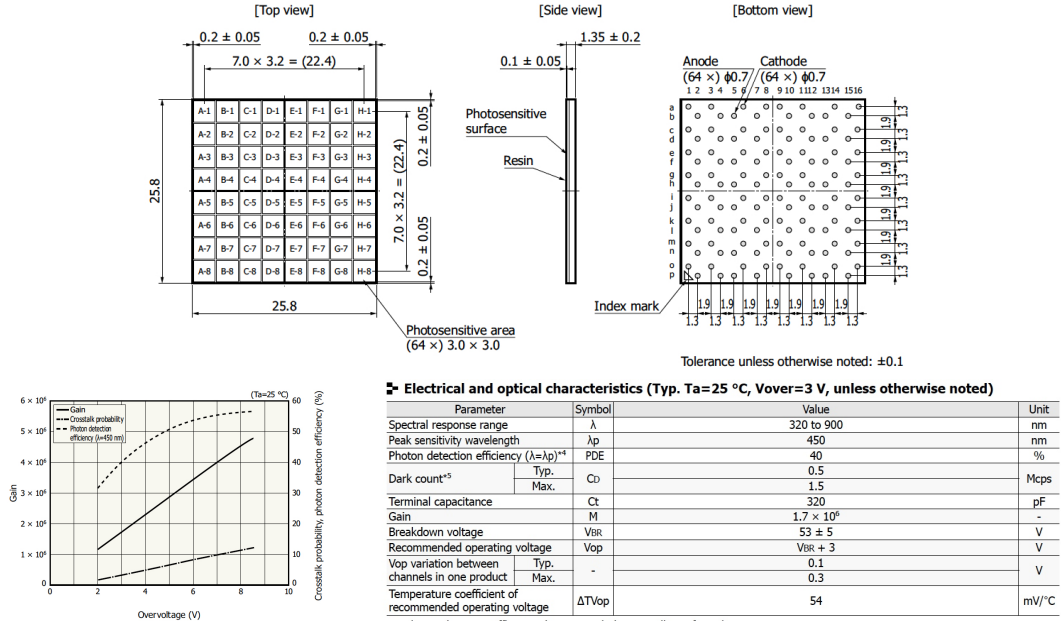


Figure 3: Above: matrix scheme and geometrical dimensions of the Hamamatsu SiPM S13161-3050AE-08 model (top, side and bottom views). Below, on the left: gain, probability of cross-talk and photon-detection efficiency as function of the over-voltage at room temperature; on the right: a table reporting electrical and optical characteristics.

temperature range; its interior size is $(300 \times 250 \times 300)$ mm³. In order to connect the EC to the instrumentations, located outside the climatic cell, 105782-120-DH-S Samtec flat cables (1 m length) are used. The EC is mounted on purpose inside a custom 3D-printed light-tight box and properly illuminated at 402 nm by a LED driver (CAEN SP5601 model), fed through a 40 cm CAEN AI2740 FC optical fiber interfaced to the box. One set-up (on the left in fig. 4) allows powering individual anodes and collect the leakage current from the cathode in the *reverse* measurement, and vice-versa in the *forward* one. A Keysight e36106b DC power supply [was used to power the EC while a Keithley 6487 pico-ammeter has been adopted for precise current measurements. Both devices were automatically operated using a specifically developed LabView program that allows setting the voltage range for supplying the EC, the stabilization time, used for stabilizing the EC after each voltage change, and the measurement time, the time interval during the current is acquired. In the second set-up (on the right, in fig. 5), the EC is directly connected to the CAEN DT5202 FERS module based on 2 Citiroc-1 A chips produced by Weeroc. The module permits carrying out photon counting, saving the signal Time Stamp and the Time over Threshold for each signal, accepting an external trigger (in such case, from the LED driver). The data acquisition is automatically operated using Janus software, an open source software specifically developed for the control and readout of FERS-5200 boards. The data archive and sharing is operated by using Notion software, an open AI (Artificial Intelligence) Workspace for archive and sharing data files, documents, plots, etc. In order to characterize the most key parameters of the ECs, all the measurements were performed at different temperatures for all 64 channels, ranging in $(-40 \div +30)$ °C with a step of 10 °C and at 25 °C with different V_{ov} . The EC characterization started evaluating V_{ov} and R_q and fixing an operating voltage for each temperature, then G, DCR and pCT are evaluated as a function of

temperature at fixed V_{ov} . A complete procedure (i.e acquisition of $(I - V)$ curves and multi-peak spectra for all the channels of a single SiPM matrix, under thermal excursions in the fixed range) for each EC require a long duration - about (10 \div 16) hours - mainly due to dead-times by the climate chamber needed for ranging to and from higher and lower temperatures. A preliminary full measurement on the first EC, in order to test the instrumentation, to validate the procedure, to fix the key parameters, to optimize the data acquisition softwares and to implement the algorithm codes for data analysis, has been successfully fulfilled (as an example, preliminary results are reported in fig.5).

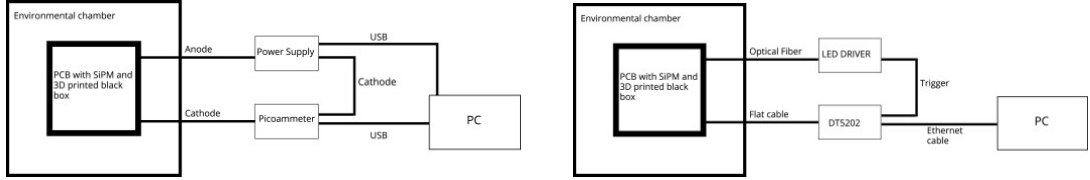


Figure 4: Left: the block diagram of the experimental set-up used for measuring the SiPM $(I - V)$ curves at different temperatures. Right: the block diagram of the experimental set-up used for measuring the SiPM multi-peak spectra at different temperatures.

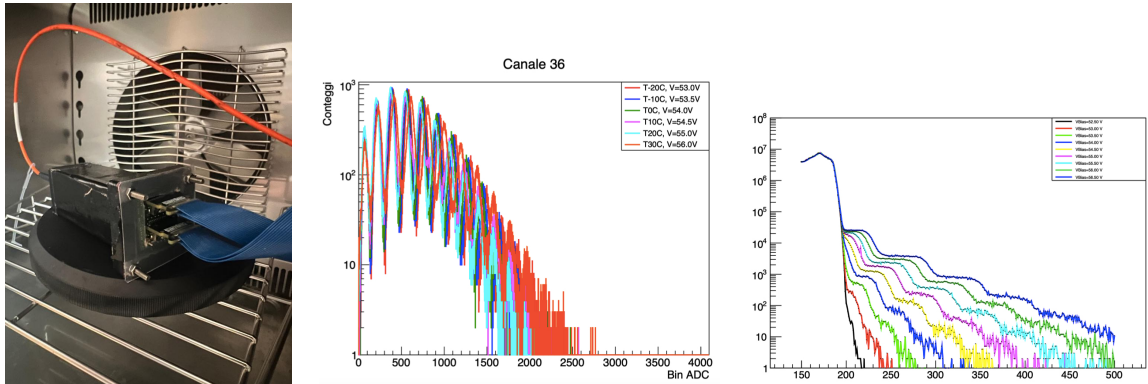


Figure 5: Left: the Elementary Cell inside the climate chamber joined to a custom 3D-printed light-tight box, placed on a designated base, illuminated by means of an optical fiber (in red) and connected with the instrumentation outside through Samtec cables (in blue); centre: multi-peak spectrum (at LED on) measured for a given channel of the first EC at fixed V_{bias} at different temperatures; right: dark count spectrum (at LED off) measured for the same given channel, at fixed temperature (25°C) for different V_{bias} .

For the time being, a fine-tuning of the whole test and calibration system is in progress, algorithm codes for analysing data are under revision, automation of the whole procedure for performing EC massive characterization is under study and the optimization of timings, based on the selection of a limited number of channels representative of the SiPM matrix, is taken into consideration.

Acknowledgments

The authors would like to acknowledge the support by NASA award 80NSSC22K1488 and 80NSSC24K1780, by the French space agency CNES and the Italian Space agency ASI. The work is supported by OP JAC financed by ESIF and the MEYS CZ.02.01.01/00/22_008/0004596. We gratefully acknowledge the collaboration and expert advice provided by the PUEO collaboration. This research used resources of the National

Energy Research Scientific Computing Center (NERSC), a U.S. Department of Energy Office of Science User Facility operated under Contract No.DE-AC02-05CH11231. We acknowledge the NASA Balloon Program Office and the Columbia Scientific Balloon Facility and staff for support. We also acknowledge the invaluable contributions of the administrative and technical staffs at our home institutions. In particular, this work would not have been possible without the financial support of the ASI-INFN agreement n. 2021-8-HH.0, its amendments and its and agreement n. 2020-26-Hh.0., Research Project “EUSO-SPB2 (Extreme Universe Space ObservatorySuper Pressure Balloon)”, WP4400 “Characterization, Selection and Test of SiPM tiles”.

References

- [1] F. Bisconti *Use of Silicon Photomultipliers in the Detectors of the JEM-EUSO Program*, *Instruments* **7** (2023) 4,55
- [2] M. Casolino, G. Cambié, L. Marcelli, E. Reali *SiPM development for space-borne and ground detectors: From Lazio-Sirad and Mini-EUSO to Lanfos*, *Nucl. Instrum. Meth. A* **986** (2021) 164649
- [3] Hamamatsu Corporation *Datasheet of S13361 Series SiPMs*, *Hamamatsu Corporation*: Hamamatsu City, Japan, 2021
- [4] R. Persiani, C. Lombardo, S. Millesoli, F. Tortorici, S. Albergo, F. Cappuzzello, R. Caruso, C.M.A. Petta, C. Tuvé *Characterization of Hamamatsu S13161-3050AE-08 SiPM (8×8) array at different temperatures with CAEN DT5202*, *Nucl.Instrum.Meth.A* **1057** (2023) 188732
- [5] R. Caruso for the ASI/INFN_EUSO-SPB2 Project *Study of performances and characterization of SiPMs (Hamamatsu S13161-3050AE-08) for the next generation of telescopes in balloon-borne and space-based experiments*, Proceedings of the Advances in Space AstroParticle Physics-2nd Edition (ASAP2025), to be published on a Special Issue of MDPI Particles
- [6] R. Caruso for the JEM-EUSO Collaboration *Overview of the JEM-EUSO Program*, Proceedings of 7th International Symposium on Ultra High Energy Cosmic Rays, *PoS(UHECR2024)* **484** (2025) 060
- [7] Z. Plebaniak for the JEM-EUSO Collaboration *From Ground to Space: An Overview of the JEM-EUSO Program for the Study of UHECRs and Astrophysical Neutrinos* *PoS(ICRC2025)* **360** (2025)
- [8] The JEM-EUSO Collaboration *EUSO-TA – First results from a ground-based EUSO telescope*, *Astropart Phys* **102** (2018) 98-111 [DOI 10.1016/j.astropartphys.2018.05.007]
- [9] J. H. Adams Jr. et al. *A Review of the EUSO-Balloon Pathfinder for the JEM-EUSO Program*, *Space Sci Rev* **218** (2022) 3 [DOI 10.1007/s11214-022-00870-x]
- [10] The JEM-EUSO Collaboration *EUSO-SPB1 mission and science*, *Astropart Phys* **154** (2024) 102891 [DOI 10.1016/j.astropartphys.2023.102891]
- [11] G. Filippatos for the JEM-EUSO Collaboration *EUSO-SPB2 Cosmic Ray Searches and Observations* *PoS(ICRC2025)* **255** (2025)
- [12] M. Battisti for the JEM-EUSO Collaboration *Five Years of Mini-EUSO Observations from the ISS: Summary of Key Results* *PoS(ICRC2025)* **183** (2025)
- [13] M. Bertaina for the JEM-EUSO Collaboration *Implications of Mini-EUSO measurements for a space-based observation of UHECRs* *PoS(ICRC2025)* **189** (2025)
- [14] J. Eser for the JEM-EUSO Collaboration *POEMMA-Balloon with Radio: An Overview* *PoS(ICRC2025)* **249** (2025)
- [15] A. V. Olinto et al. *The POEMMA (Probe of Extreme Multi-Messenger Astrophysics) Observatory*, *J COSMOL ASTROPART P* **06** (2021) 007
- [16] E. Mayotte for the JEM-EUSO Collaboration *The Optical and Mechanical Design of POEMMA Balloon with Radio* *PoS(ICRC2025)* **332** (2025)
- [17] L. Wiencke for the JEM-EUSO Collaboration *Telescope Tilt System for the POEMMA Balloon Radio Mission* *PoS(ICRC2025)* (2025)
- [18] F. Cafagna for the JEM-EUSO Collaboration *The Fluorescence Camera for the PBR mission* *PoS(ICRC2025)* **209** (2025)
- [19] V. Scotti for the JEM-EUSO Collaboration *The Cherenkov Camera for the PBR mission* *PoS(ICRC2025)* **391** (2025)
- [20] M. Bertaina for the JEM-EUSO Collaboration *Performance Results of the first version of the MIZAR ASIC for the PBR mission* *PoS(ICRC2025)* **190** (2025)

Full Authors list: The JEM-EUSO Collaboration

M. Abdullahi^{ep,er}, M. Abrate^{ek,el}, J.H. Adams Jr.^{ld}, D. Allard^{cb}, P. Alldredge^{ld}, R. Aloisio^{ep,er}, R. Ammendola^{ei}, A. Anastasio^{ef}, L. Anchordoqui^{le}, V. Andreoli^{ek,el}, A. Anzalone^{eh}, E. Arnone^{ek,el}, D. Badoni^{ei,ej}, P. von Ballmoos^{ce}, B. Baret^{cb}, D. Barghini^{ek,em}, M. Battisti^{ei}, R. Bellotti^{ea,eb}, A.A. Belov^{ia,ib}, M. Bertaina^{ek,el}, M. Betts^{lm}, P. Biermann^{da}, F. Bisconti^{ee}, S. Blin-Bondil^{cb}, M. Boezio^{ey,ez}, A.N. Bowaire^{ek,el}, I. Buckland^{ez}, L. Burmistrov^{ka}, J. Burton-Heibges^{lc}, F. Cafagna^{ea}, D. Campana^{ef,eu}, F. Capel^{db}, J. Caraca^{lc}, R. Caruso^{ec,ed}, M. Casolino^{ei,ej}, C. Cassardo^{ek,el}, A. Castellina^{ek,em}, K. Černý^{ba}, L. Conti^{en}, A.G. Coretti^{ek,el}, R. Cremonini^{ek,ev}, A. Creusot^{cb}, A. Cummings^{lm}, S. Davarpanah^{ka}, C. De Santis^{ei}, C. de la Taille^{ca}, A. Di Giovanni^{ep,er}, A. Di Salvo^{ek,el}, T. Ebisuzaki^{fc}, J. Eser^{ln}, F. Fenu^{eo}, S. Ferrarese^{ek,el}, G. Filippatos^{lb}, W.W. Finch^{lc}, C. Fornaro^{en}, C. Fuglesang^{ja}, P. Galvez Molina^{lp}, S. Garbolino^{ek}, D. Garg^{li}, D. Gardiol^{ek,em}, G.K. Garipovia^{ia}, A. Golzio^{ek,ev}, C. Guépin^{cd}, A. Haungs^{da}, T. Heibges^{lc}, F. Isgrò^{ef,eg}, R. Iuppa^{ew,ex}, E.G. Judd^{la}, F. Kajino^{fb}, L. Kupari^{li}, S.-W. Kim^{ga}, P.A. Klimov^{ia,ib}, I. Kreykenbohm^{dc}, J.F. Krizmanic^{lj}, J. Lesrel^{cb}, F. Liberatori^{ej}, H.P. Lima^{ep,er}, E. M'sihid^{cb}, D. Mandát^{bb}, M. Manfrin^{ek,el}, A. Marcelli^{ei}, L. Marcelli^{ei}, W. Marszał^{ha}, G. Masciantonio^{ei}, V. Masone^{ef}, J.N. Matthews^{lg}, E. Mayotte^{lc}, A. Meli^{lo}, M. Mese^{ef,eg,eu}, S.S. Meyer^{lb}, M. Mignone^{ek}, M. Miller^{li}, H. Miyamoto^{ek,el}, T. Montaruli^{ka}, J. Moses^{lc}, R. Munini^{ey,ez}, C. Nathan^{lj}, A. Neronov^{cb}, R. Nicolaïdis^{ew,ex}, T. Nonaka^{fa}, M. Mongelli^{ea}, A. Novikov^{lp}, F. Nozzoli^{ex}, T. Ogawa^{fc}, S. Ogio^{fa}, H. Ohmori^{fc}, A.V. Olinto^{ln}, Y. Onel^{li}, G. Osteria^{ef,eu}, B. Panico^{ef,eg,eu}, E. Parizot^{cb,cc}, G. Passeggio^{ef}, T. Paul^{ln}, M. Pech^{ba}, K. Penalo Castillo^{le}, F. Perfetto^{ef,eu}, L. Perrone^{es,et}, C. Petta^{ec,ed}, P. Picozza^{ei,ej,fc}, L.W. Piotrowski^{hb}, Z. Plebaniak^{ei}, G. Prévôt^{cb}, M. Przybylak^{hd}, H. Qureshi^{ef,eu}, E. Reali^{ei}, M.H. Renol^{li}, F. Reynaud^{ek,el}, E. Ricci^{ew,ex}, M. Ricci^{ei,ee}, A. Rivetti^{ek}, G. Saccà^{ed}, H. Sagawa^{fa}, O. Saprykin^{ic}, F. Sarazin^{lc}, R.E. Saraev^{ia,ib}, P. Schovánek^{bb}, V. Scotti^{ef,eg,eu}, S.A. Sharakin^{ia}, V. Scherini^{es,et}, H. Schieler^{da}, K. Shinozaki^{ha}, F. Schröder^{lp}, A. Sotgiu^{ei}, R. Sparvoli^{ei,ej}, B. Stillwell^{lb}, J. Szabelski^{hc}, M. Takeda^{fa}, Y. Takizawa^{fc}, S.B. Thomas^{lg}, R.A. Torres Saavedra^{ep,er}, R. Triggiani^{ea}, D.A. Trofimov^{ia}, M. Unger^{da}, T.M. Venters^{lj}, M. Venugopal^{da}, C. Vigorito^{ek,el}, M. Vrabel^{ha}, S. Wada^{fc}, D. Washington^{lm}, A. Weindl^{da}, L. Wiencke^{lc}, J. Wilms^{dc}, S. Wissel^{lm}, I.V. Yashin^{ia}, M.Yu. Zotov^{ia}, P. Zuccon^{ew,ex}.

^{ba} Palacký University, Faculty of Science, Joint Laboratory of Optics, Olomouc, Czech Republic

^{bb} Czech Academy of Sciences, Institute of Physics, Prague, Czech Republic

^{ca} École Polytechnique, OMEGA (CNRS/IN2P3), Palaiseau, France

^{cb} Université de Paris, AstroParticule et Cosmologie (CNRS), Paris, France

^{cc} Institut Universitaire de France (IUF), Paris, France

^{cd} Université de Montpellier, Laboratoire Univers et Particules de Montpellier (CNRS/IN2P3), Montpellier, France

^{ce} Université de Toulouse, IRAP (CNRS), Toulouse, France

^{da} Karlsruhe Institute of Technology (KIT), Karlsruhe, Germany

^{db} Max Planck Institute for Physics, Munich, Germany

^{dc} University of Erlangen–Nuremberg, Erlangen, Germany

^{ea} Istituto Nazionale di Fisica Nucleare (INFN), Sezione di Bari, Bari, Italy

^{eb} Università degli Studi di Bari Aldo Moro, Bari, Italy

^{ec} Università di Catania, Dipartimento di Fisica e Astronomia “Ettore Majorana”, Catania, Italy

^{ed} Istituto Nazionale di Fisica Nucleare (INFN), Sezione di Catania, Catania, Italy

^{ee} Istituto Nazionale di Fisica Nucleare (INFN), Laboratori Nazionali di Frascati, Frascati, Italy

^{ef} Istituto Nazionale di Fisica Nucleare (INFN), Sezione di Napoli, Naples, Italy

^{eg} Università di Napoli Federico II, Dipartimento di Fisica “Ettore Pancini”, Naples, Italy

^{eh} INAF, Istituto di Astrofisica Spaziale e Fisica Cosmica, Palermo, Italy

^{ei} Istituto Nazionale di Fisica Nucleare (INFN), Sezione di Roma Tor Vergata, Rome, Italy

^{ej} Università di Roma Tor Vergata, Dipartimento di Fisica, Rome, Italy

ek Istituto Nazionale di Fisica Nucleare (INFN), Sezione di Torino, Turin, Italy
el Università di Torino, Dipartimento di Fisica, Turin, Italy
em INAF, Osservatorio Astrofisico di Torino, Turin, Italy
en Università Telematica Internazionale UNINETTUNO, Rome, Italy
eo Agenzia Spaziale Italiana (ASI), Rome, Italy
ep Gran Sasso Science Institute (GSSI), L'Aquila, Italy
er Istituto Nazionale di Fisica Nucleare (INFN), Laboratori Nazionali del Gran Sasso, Assergi, Italy
es University of Salento, Lecce, Italy
et Istituto Nazionale di Fisica Nucleare (INFN), Sezione di Lecce, Lecce, Italy
eu Centro Universitario di Monte Sant'Angelo, Naples, Italy
ev ARPA Piemonte, Turin, Italy
ew University of Trento, Trento, Italy
ex INFN–TIFPA, Trento, Italy
ey IFPU – Institute for Fundamental Physics of the Universe, Trieste, Italy
ez Istituto Nazionale di Fisica Nucleare (INFN), Sezione di Trieste, Trieste, Italy
fa University of Tokyo, Institute for Cosmic Ray Research (ICRR), Kashiwa, Japan
fb Konan University, Kobe, Japan
fc RIKEN, Wako, Japan
ga Korea Astronomy and Space Science Institute, South Korea
ha National Centre for Nuclear Research (NCBJ), Otwock, Poland
hb University of Warsaw, Faculty of Physics, Warsaw, Poland
hc Stefan Batory Academy of Applied Sciences, Skierniewice, Poland
hd University of Lodz, Doctoral School of Exact and Natural Sciences, Łódź, Poland
ia Lomonosov Moscow State University, Skobeltsyn Institute of Nuclear Physics, Moscow, Russia
ib Lomonosov Moscow State University, Faculty of Physics, Moscow, Russia
ic Space Regatta Consortium, Korolev, Russia
ja KTH Royal Institute of Technology, Stockholm, Sweden
ka Université de Genève, Département de Physique Nucléaire et Corpusculaire, Geneva, Switzerland
la University of California, Space Science Laboratory, Berkeley, CA, USA
lb University of Chicago, Chicago, IL, USA
lc Colorado School of Mines, Golden, CO, USA
ld University of Alabama in Huntsville, Huntsville, AL, USA
le City University of New York (CUNY), Lehman College, Bronx, NY, USA
lg University of Utah, Salt Lake City, UT, USA
li University of Iowa, Iowa City, IA, USA
lj NASA Goddard Space Flight Center, Greenbelt, MD, USA
lm Pennsylvania State University, State College, PA, USA
ln Columbia University, Columbia Astrophysics Laboratory, New York, NY, USA
lo North Carolina A&T State University, Department of Physics, Greensboro, NC, USA
lp University of Delaware, Bartol Research Institute, Department of Physics and Astronomy, Newark, DE, USA